

Nitrous oxide (N₂O) emissions from a mesotrophic reservoir on the Wujiang River, southwest China

Xiaolong Liu¹  · Siliang Li² · Zhongliang Wang¹ · Guilin Han³ · Jun Li¹ · Baoli Wang² · Fushun Wang⁴ · Li Bai¹

Received: 16 January 2017 / Revised: 21 February 2017 / Accepted: 24 April 2017 / Published online: 10 May 2017
© Science Press, Institute of Geochemistry, CAS and Springer-Verlag Berlin Heidelberg 2017

Abstract Aquatic ecosystems have been identified as a globally significant source of nitrous oxide (N₂O) due to continuous active nitrogen involvement, but the processes and influencing factors that control N₂O production are still poorly understood, especially in reservoirs. For that, monthly N₂O variations were monitored in Dongfeng reservoir (DFR) with a mesotrophic condition. The dissolved N₂O concentration in DFR displayed a distinct spatial–temporal pattern but lower than that in the eutrophic reservoirs. During the whole sampling year, N₂O saturation ranging from 144% to 640%, indicating that reservoir acted as source of atmospheric N₂O. N₂O production is induced by the introduction of nitrogen (NO₃[−], NH₄⁺) in mesotrophic reservoirs, and is also affected by oxygen level and water temperature. Nitrification was the predominate process for N₂O production in DFR due to well-oxygenated longitudinal water layers. Mean values of estimated N₂O flux from the air–water interface averaged 0.19 μmol m^{−2} h^{−1} with a range of 0.01–0.61 μmol m^{−2} h^{−1}. DFR exhibited less N₂O

emission flux than that reported in a nearby eutrophic reservoir, but still acted as a moderate N₂O source compared with other reservoirs and lakes worldwide. Annual emissions from the water–air interface of DFR were estimated to be 0.32 × 10⁵ mol N–N₂O, while N₂O degassing from releasing water behind the dam during power generation was nearly five times greater. Hence, N₂O degassing behind the dam should be taken into account for estimation of N₂O emissions from artificial reservoirs, an omission that historically has probably resulted in underestimates. IPCC methodology should consider more specifically N₂O emission estimation in aquatic ecosystems, especially in reservoirs, the default EF5 model will lead to an overestimation.

Keywords Nitrous oxide · Mesotrophic reservoir · Nitrogen dynamics · IPCC methodology

1 Introduction

River impoundment and dam construction have significantly altered the aquatic environment and water dynamics during recent decades, resulting in complex feedback mechanisms on nitrogen biogeochemical cycles. In 1996, there were approximately 42000 large dams in rivers worldwide (Rosenberg et al. 2000). Hydroelectric power was accepted as “green energy” for a long time, but in recent years researchers have noted associated deterioration of water quality and aquatic environments, including eutrophication and greenhouse gas (GHG) emissions (Liu et al. 2011a; Wang et al. 2011; Beaulieu et al. 2015; Fearnside 2016). Indeed, most of the hydroelectric reservoirs worldwide have been identified as potentially important sources GHGs, including CO₂, CH₄, and nitrous oxide (N₂O) (Peng et al. 2012; Sturm et al. 2014; Beaulieu

✉ Xiaolong Liu
liu_xiaolong@126.com

✉ Siliang Li
siliang.li@tju.edu.cn

¹ Tianjin Key Laboratory of Water Resources and Environment, Tianjin Normal University, Tianjin 300387, China

² Institute of Surface-Earth System Science, Tianjin University, Tianjin 300072, China

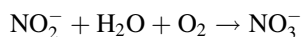
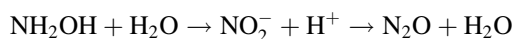
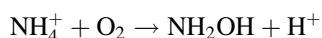
³ School of Scientific Research, China University of Geosciences (Beijing), Beijing 100083, China

⁴ Applied Radiation Institute, School of Environmental and Chemical Engineering, Shanghai University, Shanghai 200433, China

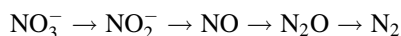
et al. 2015; Fearnside 2016; Musenze et al. 2016). Aquatic N₂O production and emissions at reservoirs have attracted additional attention recently as increased nitrogen loading in reservoirs has resulted from anthropogenic activity (Beaulieu et al. 2015).

N₂O, a powerful GHG that contributes significantly to the destruction of stratospheric ozone (Ravishankara et al. 2009), is an important component of nitrogen loss during aquatic nitrogen biogeochemical cycling. Although atmospheric N₂O concentration is lower than CO₂, its global warming potential is about 298 times greater than CO₂ (IPCC 2006). Atmospheric mixing ratios of N₂O have been increasing steadily over the past century. Aquatic systems contribute 25%–30% of total global N₂O emissions (IPCC 2006).

N₂O is mainly produced during microbial processes such as nitrification and denitrification. Nitrification is an aerobic process through which ammonium is oxidized to nitrate. During this process, N₂O is a by-product of the oxidation of NH₄⁺ by nitrifying bacteria and methanotrophs (Mengis et al. 1997). The yield of N₂O in nitrification strongly depends on the concentrations of dissolved oxygen and nitrate. The processing steps of nitrification are:



In suboxic conditions, nitrate can be reduced by denitrification to molecular nitrogen, with N₂O as an intermediate. The rate of denitrification is influenced by temperature, abundance of organic carbon, and supply of N. As an intermediate in denitrification (NO₃[−] to N₂), N₂O may accumulate when O₂ is present along with high NO₃[−] concentrations:



Nitrification and denitrification often occur simultaneously in aquatic ecosystems, especially in periodically thermally stratified deep reservoirs (depth >30 m) (Liu et al. 2011a; Beaulieu et al. 2015). Factors controlling N₂O yield, including temperature, available dissolved oxygen, nitrogen variation, and organic matter, vary temporally and spatially in reservoirs, and little is known about their specific impacts on N₂O yield in reservoirs. While N₂O is enhanced by increasing N levels and increasing eutrophication, this connection is not well characterized. Reservoirs are complex and dynamic ecosystems and it is important to understand how they operate and respond to changes in order to make appropriate management decisions.

Calculated N₂O emissions from China are globally significant, accounting for over 90% of those in the Pacific

Basin (Seitzinger and Kroeze 1998), but there is still considerable uncertainty or overestimation as few studies of N₂O production and emission have been made in China's reservoirs (Liu 2007; Liu et al. 2011a). The objectives of our study are: (1) to ascertain the spatial and temporal variations of N₂O emission and assess whether the reservoir functions as a sink or a source of N₂O, (2) to understand the impact of nitrogen dynamics on N₂O emissions, and (3) to assess the production mechanisms of N₂O and influential factors.

2 Study area and methods

2.1 Study area

The Wujiang is one of the largest tributaries in the upper reaches of the Changjiang Basin, mainly flowing through a karst area in Guizhou Province, with a total length of 874 km, drainage area of 66849 km², and mean water discharge of 1690 m³ s^{−1}. The karst landscape accounts for about 70% of the total drainage area of the Wujiang River, and water chemistry is controlled by carbonate dissolution under the influence of carbonic and sulfuric acid (Han et al. 2010). The region experiences a subtropical monsoon humid climate, with perennial mean temperature of 14.8 °C and multi-year average annual rainfall of about 1100 mm. Dongfeng reservoir (DFR) (26°51'N, 106°8'E), located in Qingzhen City, Guizhou Province, was completed in 1994. It has a surface area of 19.06 km², a total volume of 8.63 × 10⁸ m³, and drainage area of 18161 km².

2.2 Sampling

Samples were collected monthly from July 2007 to June 2008 (Fig. 1) from the central part of the river, generally 0.4–0.5 km upstream of the dam at depths of 0.5, 5, 15, 30, and 60 m using a Niskin bottle. Samples downstream of the dam were collected 0.5 m under the water surface. In total, 60 vertical samples and 12 downstream samples were collected.

2.3 Environmental variables and nitrogen species

Water temperature (T), pH, dissolved oxygen (DO), and chlorophyll levels were measured in situ using an automated multi-parameter monitoring instrument (United States Gimcheon Instruments Inc. YSI 6600 v2). Water samples were filtered through 0.70-μm membrane filters (Whatman), H₂SO₄ was added (pH < 2), and the samples were cold-stored at <4 °C in the dark until analyzed. The concentrations of NO₃[−] were measured using an automatic flow analyzer (SKALAR Sans Plus Systems), with

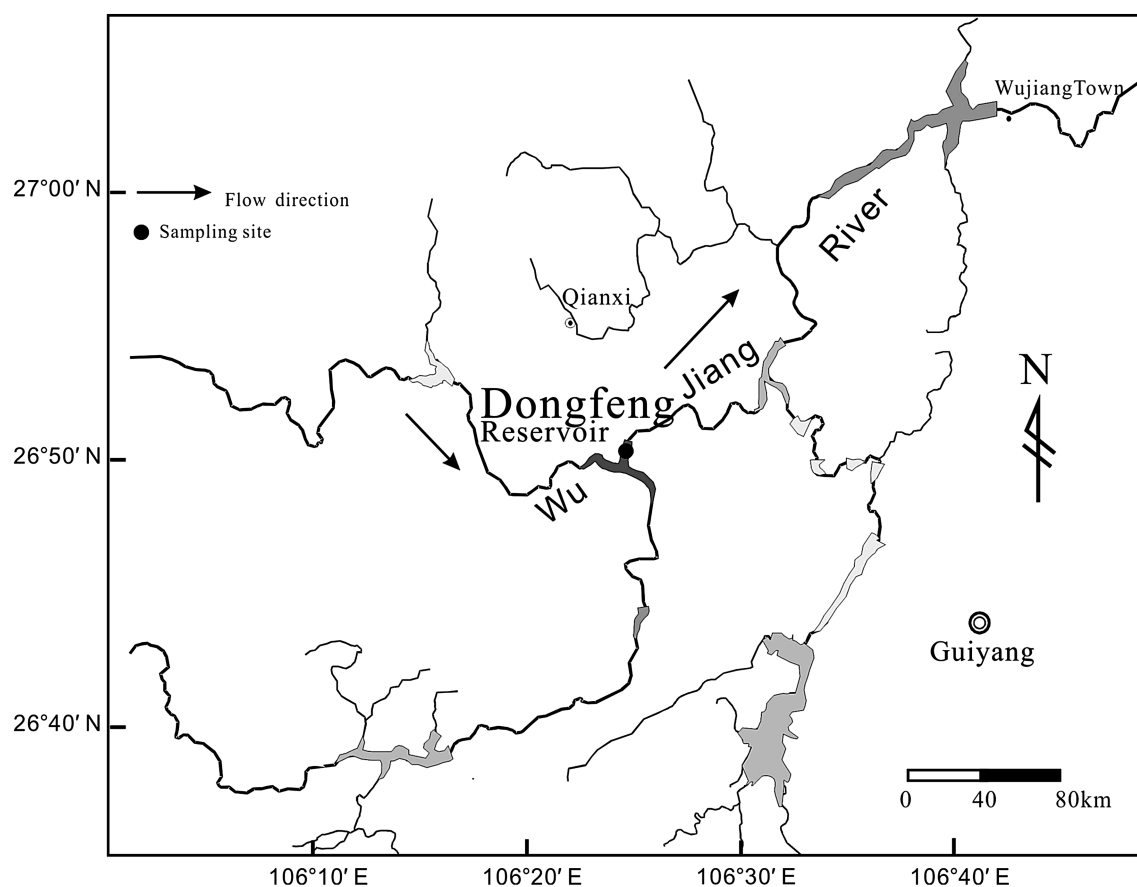


Fig. 1 Map showing the location of Dongfeng reservoir on the Wujiang River

precision under 2% as determined by duplicate samples. In addition, total phosphorous (TP) was determined spectrophotometrically (Unico UV-2000) using the molybdenum blue method after alkaline potassium persulfate digestion. Total nitrogen (TN) was also analyzed spectrophotometrically (Unico UV-2000) after alkaline potassium persulfate digestion. The typical precision of TN and TP measured by the spectrophotometric method is $\pm 3\%$.

2.4 N₂O measurement and flux calculation

N₂O concentration in water was measured following the headspace-GC method. Water samples were collected in serum bottles, amended with 10 mol L⁻¹ sodium hydroxide (NaOH) as a preservative, and sealed with rubber stoppers. The headspace equilibrium technique was used to determine the concentrations of dissolved gases. Details are available in Liu et al. (2011a) and Wang et al. (2009). The relative errors for N₂O measurement were less than 2%; regression corrections with ambient air were less than ± 10 nmol L⁻¹.

For assessing N₂O concentration and saturation, gas concentrations were expressed as the degree of saturation relative to air (Mengis et al. 1997):

$$\text{Degree of N}_2\text{O}_{\text{saturation}} = C_{\text{N}_2\text{O}}/C_{\text{N}_2\text{Oatm}} \times 100 \quad (1)$$

$$C_{\text{N}_2\text{Oatm}} = K \times C_A \quad (2)$$

where $C_{\text{N}_2\text{O}}$ is the measured concentration, $C_{\text{N}_2\text{Oatm}}$ is the saturated concentration of N₂O in water at the given water temperature and C_A is the atmospheric N₂O concentration of the sampling sites. The saturated concentration of N₂O in water was calculated using Henry's Law, where K is the Bunsen coefficient.

Apparent oxygen utilization (AOU) and $\Delta\text{N}_2\text{O}$ were calculated as follows:

$$\text{AOU} = \text{DO}_{\text{sat}} - \text{DO}_{\text{meas}} \quad (3)$$

$$\Delta\text{N}_2\text{O} = C_{\text{N}_2\text{O}} - C_{\text{N}_2\text{Oatm}} \quad (4)$$

where DO_{sat} is the saturation DO concentration in water and DO_{meas} is the measured concentration of DO.

The exchange flux of N₂O at the gas–water boundary layer of the surface water was calculated as:

$$F = K\Delta C = \frac{D}{Z}(C_s - C_{eq}) \quad (5)$$

$$D = 5.06 \times 10^{-9} \frac{T}{\eta V_b^{0.6}} \quad (6)$$

where F is the gas exchange flux; ΔC is the difference between the N_2O concentration in the air and water; K is the gas transfer velocity; D is the gas diffusion coefficient, which was calculated using Eq. (6), obtained from Lerman (1979); η is the viscosity of the water; V_b is the molar volume of the gas, with a value of $36.4 \text{ cm}^3 \text{ mol}^{-1}$ (Satterfield 1970); and Z is the thickness of the boundary layer, which is an empirical constant related to wind speed (Emerson 1975). Taking into account variations in wind speed for each sampling month, Z was estimated to have a value of 180–350 μm .

2.5 Statistical analysis

Statistical analysis was conducted using SPSS Statistics 22.0.0, Grapher 12.0, and Microsoft Excel in Windows 10. In all analyses where $p < 0.05$, the factor and the relationship tested were considered statistically significant.

3 Results

3.1 Variation of water parameters and trophic status

Surface water parameters including temperature, pH, chlorophyll, and DO displayed significant monthly variation (Fig. 2). Monthly variation data were divided into two groups: cold season (November to March) and warm season (April to October). DO, pH, and chlorophyll in the cold season ranged from 188.75 to 323.75 $\mu\text{mol L}^{-1}$ (average 281.65 $\mu\text{mol L}^{-1}$), 7.50–8.73 (average 7.83), and 0.01–2.20 $\mu\text{g L}^{-1}$ (average 0.24 $\mu\text{g L}^{-1}$), respectively. In warm season, DO, pH, and chlorophyll ranged from 209.69 to 337.50 $\mu\text{mol L}^{-1}$ (average 271.38 $\mu\text{mol L}^{-1}$), 7.25–8.73 (average 7.88), and 0.05–6.60 $\mu\text{g L}^{-1}$ (0.93 $\mu\text{g L}^{-1}$), respectively. All three parameters were generally higher in the warm season than in the cold season. Temperature, pH, DO, and chlorophyll in DFR surface waters shared similar seasonal trends with the Hongjiadu (HJD) and Wujiangdu (WJD) reservoirs on the mainstem of the Wujiang River (Liu et al. 2011a) and with reservoirs in the Maotiao River (Wang et al. 2011, 2015). However, DFR had higher DO and lower pH than HJD; and lower DO, pH, and chlorophyll than WJD.

DFR was typically thermally stratified in spring (April to June) and summer (July to September) during the sampling year. Thermal stratification was absent from October to March (Fig. 4). pH and DO showed similar vertical

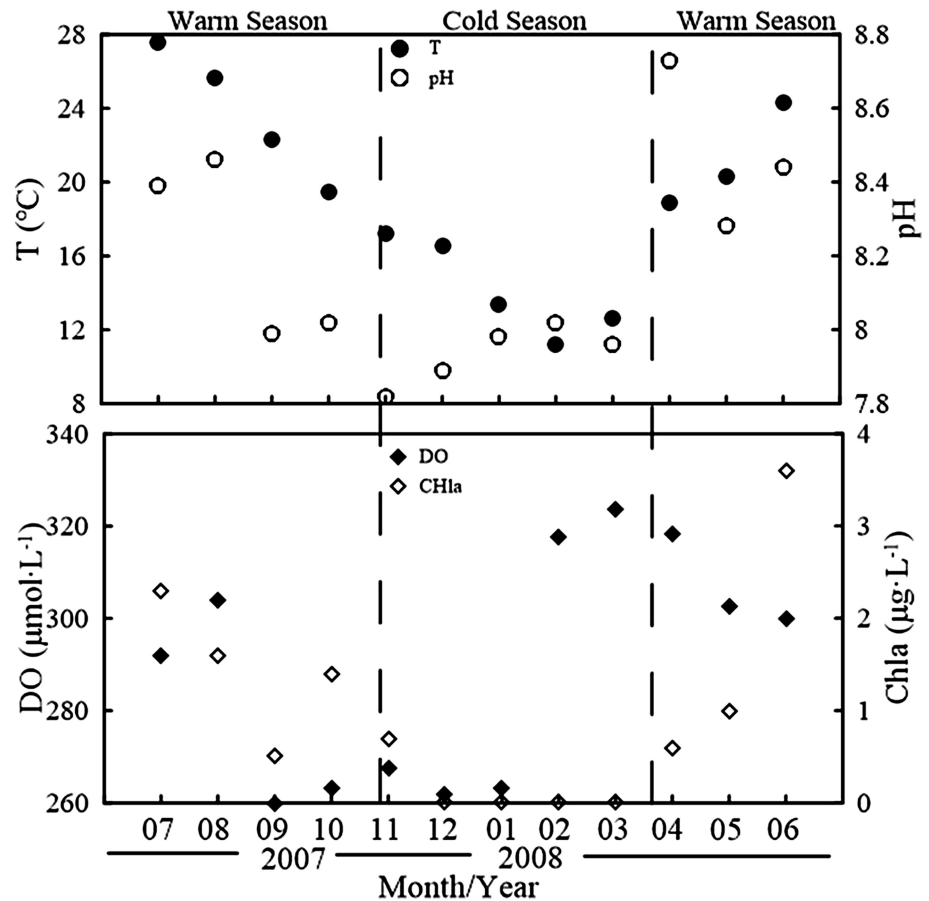
distribution. In thermally stratified months, pH and DO values were lower in the deep water layers than in surface waters, e.g. mean values of 7.69 and 242.14 $\mu\text{mol L}^{-1}$, respectively, in the bottom layer, and of 8.38 and 296.15 $\mu\text{mol L}^{-1}$ in surface waters. Compared with HJD and WJD, pH and DO in the bottom layer of DFR were much higher (Liu et al. 2011a), perhaps because DFR is much deeper (>100 m) than the others. DO data suggest that deep waters (depth of 60 m) maintained anoxic environment.

Results for TN, TP, and chlorophyll concentrations are in Fig. 3. TN and TP in DFR surface waters ranged from 2.30 to 5.11 mg L^{-1} (average 3.50 mg L^{-1}) and 0.001–0.31 mg L^{-1} (average 0.04 mg L^{-1}), respectively. Significant monthly variation in TP and chlorophyll were observed, suggesting eutrophic status varied greatly between cold seasons and warm seasons. DFR had moderate TN, TP, and chlorophyll content when compared with HJD and WJD (Liu et al. 2011a). However, as discussed and reported previously, reservoirs along Wujiang River have higher nitrogen loading than other reservoirs, such as Harsha Lake (Beaulieu et al. 2014), and Three Gorges reservoir (Zhu et al. 2013). Comparable high nitrogen loading has been reported in other watersheds and reservoirs, such as Brookville Lake and Mississinewa (Beaulieu et al. 2015). The main nitrate sources in the Wujiang watershed are nitrification and flooded soil organic matter (Li et al. 2010). The moderate levels of TN, TP, and chlorophyll in DFR indicate that the reservoir has a mesotrophic nutrient status when compared to its upstream (HJD) and downstream (WJD) counterparts. Chlorophyll was only detected in the upper layer (>15 m); average concentrations in thermal stratification months and non-thermal stratification months were 2.23 and 0.46 $\mu\text{g L}^{-1}$, respectively. In comparison, chlorophyll in WJD and HJD in the warm season averaged 20.45 and 2.66 $\mu\text{g L}^{-1}$, respectively, and in the cold season, 1.01 and 0.53 $\mu\text{g L}^{-1}$. The concentration of chlorophyll in DFR is very similar to HJD, an oligotrophic reservoir, but is notably lower than WJD, a eutrophic reservoir.

3.2 Monthly and spatial variation of N_2O in the reservoir

Significant vertical and monthly variation of N_2O concentration was observed in DFR (Fig. 3). All surface waters were supersaturated with respect to the equilibrium atmospheric N_2O concentration, 319 ppbv (IPCC 2006). The N_2O concentration in surface waters ranged from 15.05 to 59.63 nmol L^{-1} (average 27.03 nmol L^{-1}); corresponding N_2O saturations were from 164.79% to 640.89% (average 287.31%), indicating that DFR represents a N_2O source to the atmosphere.

Fig. 2 Monthly variations of environmental variables in surface waters



Significant vertical variation of N_2O was observed throughout the sampling year. Monthly average N_2O concentration in the deep water (depth >30 m) was significantly higher than that in surface waters (t test, $p < 0.05$), except in April and February. These anomalies were possibly due to N_2O accumulation in the hypolimnion where gas diffusion was constrained by the water density gradient. There was no apparent seasonal variation pattern of N_2O throughout the sampling year (Fig. 4). In the cold season, average surface-water N_2O concentration was $26.02 \text{ nmol L}^{-1}$, while in the warm season it was $28.03 \text{ nmol L}^{-1}$. Longitudinal averaged N_2O concentration in the cold season was $28.40 \text{ nmol L}^{-1}$, in contrast with $30.11 \text{ nmol L}^{-1}$ in the warm season.

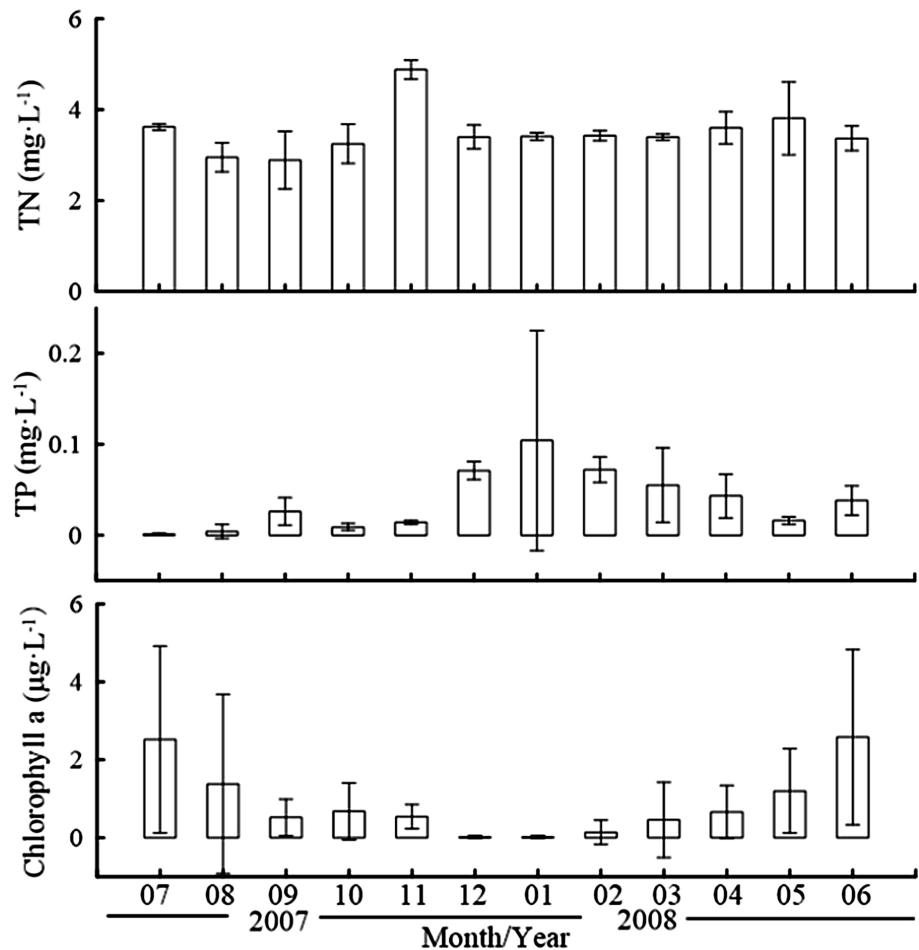
In general, N_2O concentration and saturation in DFR were conspicuously lower than in the WJD reservoir and slightly higher than in the HJD reservoir (Liu et al. 2011a). As previously noted, DFR is classified as a mesotrophic reservoir while HJD is oligotrophic and WJD eutrophic, suggesting that N_2O concentration may differ according to nutrient status, with eutrophic having the highest N_2O saturation potential. This is coincident with the findings in Swiss lakes and reservoirs by Mengis et al. (1997), who concluded that oligo-

mesotrophic reservoirs had significantly lower N_2O saturation than eutrophic ones. In addition, DFR had slightly higher N_2O concentration and saturation than Ohio River basin oligotrophic reservoirs ($4 < \text{NO}_{2,3} < 19 \text{ } \mu\text{g N L}^{-1}$; N_2O saturation ratio 0.4–2.0), but significantly lower than Ohio River basin mesotrophic and eutrophic reservoirs ($16 < \text{NO}_{2,3} < 1786 \text{ } \mu\text{g N L}^{-1}$; N_2O saturation ratio 0–1000) (Beaulieu et al. 2014).

3.3 N_2O diffusion fluxes

Conservative estimates of N_2O flux in DFR were based on wind speed data provided by the meteorological observatory and on surface water N_2O saturation (Fig. 5). Monthly N_2O flux on the water–air interface ranged from 0.01 to $0.61 \text{ } \mu\text{mol m}^{-2} \text{ h}^{-1}$, with an average value of $0.19 \text{ } \mu\text{mol m}^{-2} \text{ h}^{-1}$. The highest emission flux was in April, while the lowest was in October, both turnover months between thermal and non-thermal stratified periods. No obvious seasonal difference in N_2O flux was exhibited. Compared to the average surface flux in surface waters of adjacent reservoirs WJD and HJD ($0.67 \text{ } \mu\text{mol m}^{-2} \text{ h}^{-1}$ and $0.45 \text{ } \mu\text{mol m}^{-2} \text{ h}^{-1}$, respectively), DFR had notably lowest emission level of the three reservoirs.

Fig. 3 Monthly variation of TN, TP, and Chlorophyll in Dongfeng reservoir



4 Discussion

4.1 Effects of nitrogen and environment variables on N₂O

Environmental variables such as T, DO, and nitrogen species are known to influence N₂O production and emissions in artificial reservoirs (Liu et al. 2011a; Zhu et al. 2013; Beaulieu et al. 2014, 2015). The relationships between N₂O concentration and nitrogen species, T, and DO in DFR were analyzed (Fig. 6); T and DO were recognized as the two most important factors for spatial and temporal N₂O variation. T was found to have a significant negative correlation with N₂O concentration in summer and spring ($R = 0.55$; $P = 0.003$), while a positive correlation in winter ($R = 0.70$; $P = 0.004$). DO in DFR also had a negative correlation with N₂O in summer and autumn ($R = 0.63$; $P < 0.001$), while a positive correlation in spring ($R = 0.60$; $P = 0.002$). Seasonal differences in the relationships of T and DO with N₂O may be related to the complexity of N₂O production throughout the water column. T exhibited an opposite correlation with N₂O in warm seasons versus winter probably due to significant differences of N₂O between

surface waters and deep waters in warm seasons while this phenomena disappeared in winter (Fig. 4). Good correlation between T and N₂O in surface waters was also found in Three Gorges reservoir (Zhu et al. 2013), but this correlation has not held in other reservoirs worldwide (Huttunen et al. 2002; Hendzel et al. 2005; Guerin et al. 2008; Liu et al. 2011a; Zhu et al. 2013; Beaulieu et al. 2014). Actually, N₂O production mainly occurs in the water column in reservoirs, especially in the hypolimnion (Deemer et al. 2011; Beaulieu et al. 2014), thus the influence of temperature and DO on N₂O production also depends on other parameters such as nitrogen loading in water layers and dissolved organic carbon content.

The relationships of N₂O with NO₃⁻ and NH₄⁺ in different seasons were analyzed at DFR (Fig. 6). We found a good and positive relationship between N₂O and NO₃⁻ in autumn ($R = 0.63$; $P = 0.016$), with the exception of one deep-water sample at 60 m (Fig. 6). Positive correlations between N₂O and NO₃⁻ are well documented in rivers and streams (Yu et al. 2013; Liu et al. 2015), lakes (Wang et al. 2009), and reservoirs (Liu et al. 2011a; Beaulieu et al. 2015). Nitrification and denitrification have been identified as the major N₂O-producing pathways in reservoirs (Mengis et al. 1997; Deemer et al. 2011; Liu et al. 2011a;

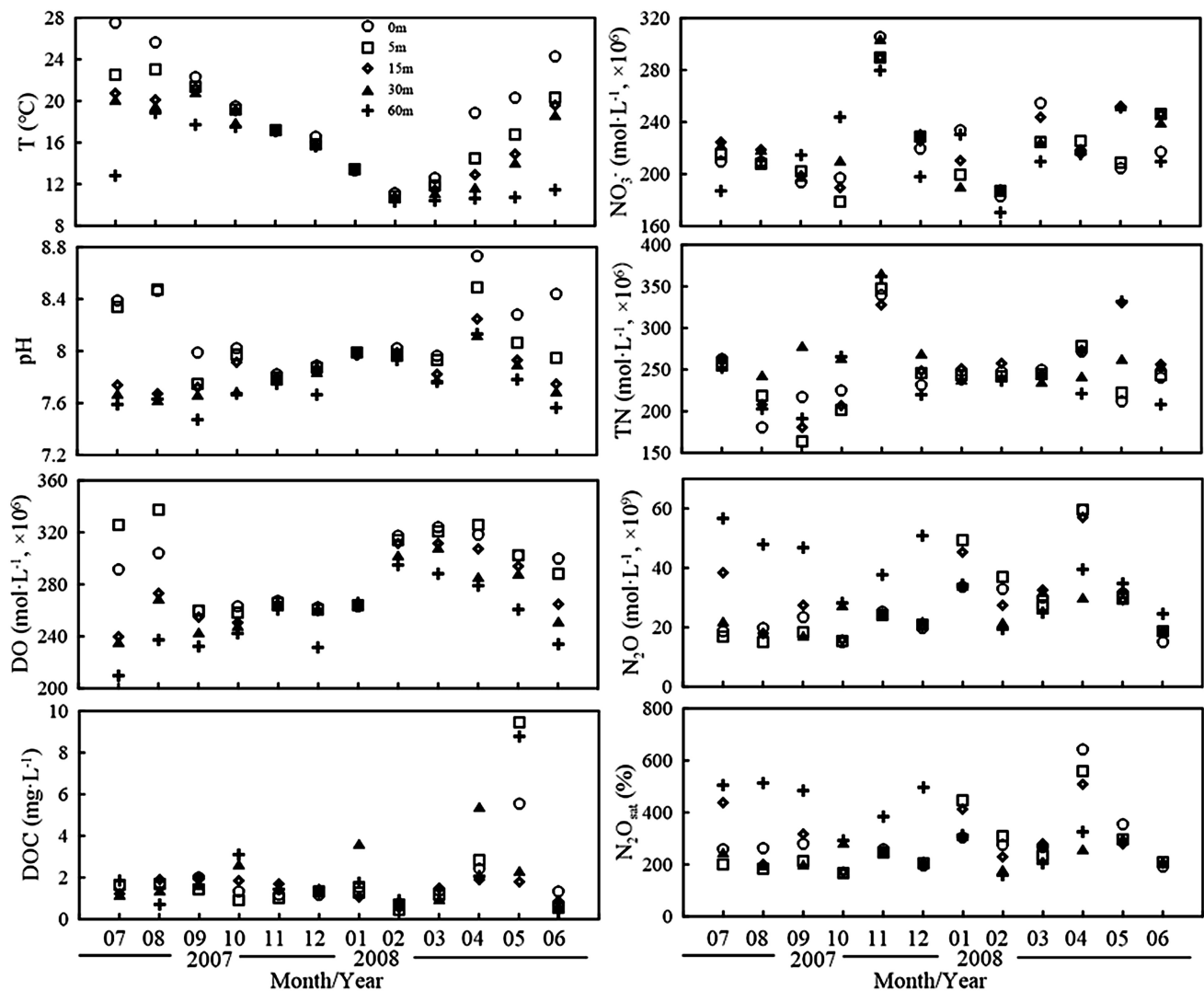


Fig. 4 Longitudinal and monthly distribution pattern of N_2O and main parameters

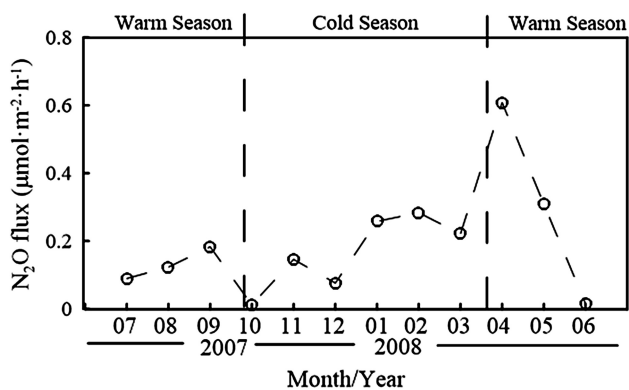


Fig. 5 N_2O concentration, saturation, and emission flux in surface waters

Beaulieu et al. 2014), and NO_3^- should have a positive correlation with N_2O , especially in nitrification-dominated aquatic environments. However, in DFR, a significant

relationship was observed between N_2O and NO_3^- only in autumn, which was likely due to N_2O being produced by both nitrification and denitrification, resulting in disproportionate NO_3^- consumption and production with N_2O production. Excess NO_3^- and exogenous nitrogen input into a reservoir also result in this disproportionation.

A positive correlation between N_2O and NH_4^+ ($R = 0.82$; $P < 0.001$) was identified in the warm season (from April to September) with a slope of 1.13 (Fig. 6). As previously noted, the water column remained oxic throughout the year, even during the thermal stratification period. A well-oxygenated water column provides ideal conditions for NH_4^+ oxidation. The first step of nitrification is the oxidation of NH_4^+ to hydroxylamine (NH_2OH), during which both NO_2^- and N_2O are produced. If the NO_2^- is not immediately oxidized to NO_3^- , reduced to N_2O or N_2 (nitrifier-denitrification), or assimilated into biomass, NH_4^+ oxidation results in the simultaneous

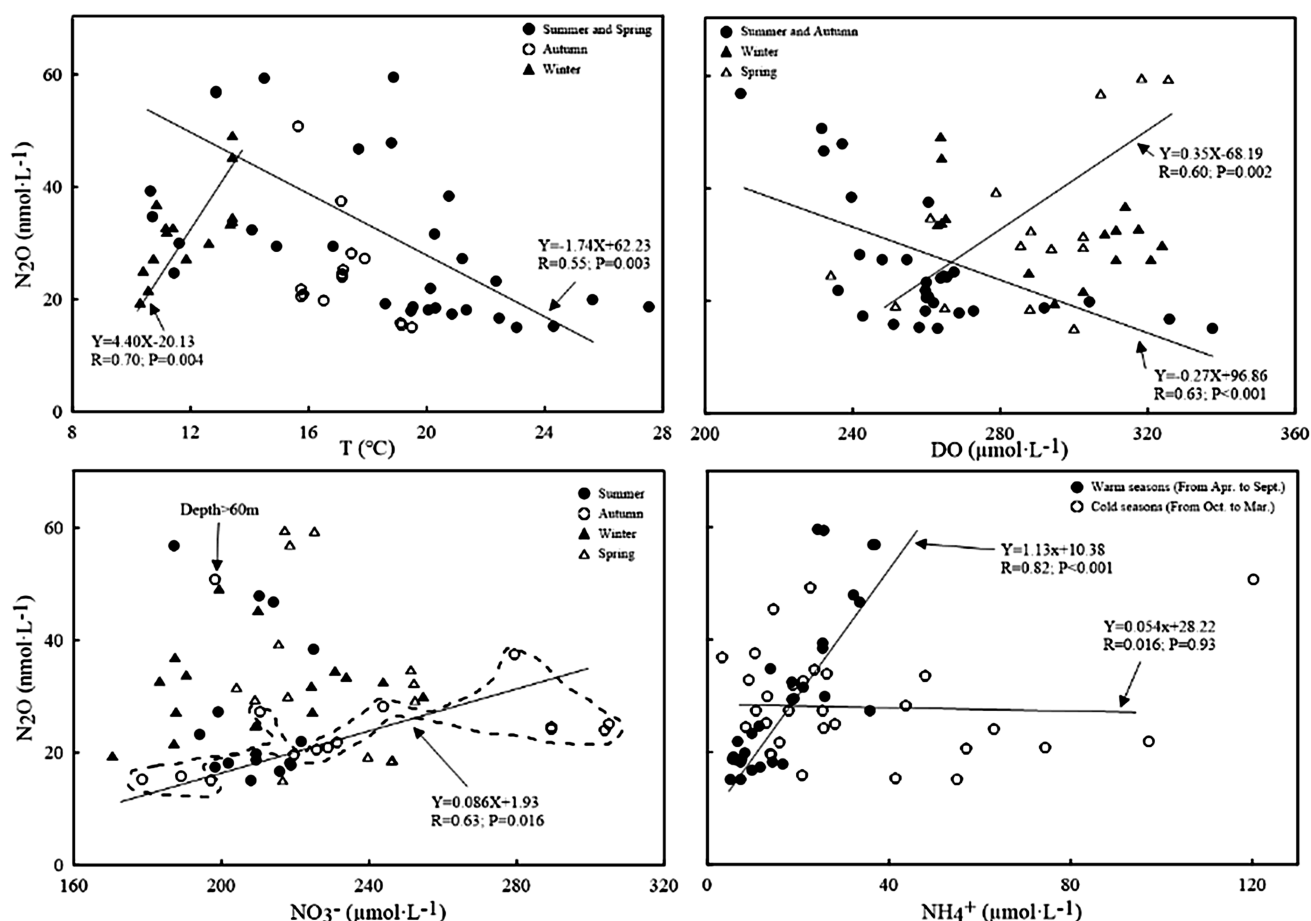


Fig. 6 Correlation of N_2O with nitrogen and T, DO in Dongfeng reservoir

accumulation of N_2O and NO_2^- (Sasaki et al. 2011; Beaulieu et al. 2015). In other words, NH_4^+ promotes N_2O production in oxygenated water layers when sufficient NH_4^+ is available. But in cold seasons, the mineralization process, which produces NH_4^+ through organic matter decomposition in anaerobic water layers, would be blocked by well-oxygenated waters and water-mixing processes.

4.2 Production mechanisms of N_2O

As previously noted, denitrification is not a dominant process for N_2O production, but how it might influence spatial and temporal N_2O distribution in DFR still unknown. That is to say, whether nitrification is solely responsible for N_2O in this mesotrophic reservoir remains to be determined. A linear correlation between $\Delta\text{N}_2\text{O}$ and AOU in oxic waters has established that N_2O is produced by nitrification in oceans, lakes, rivers, and reservoirs. AOU reflects the amount of O_2 consumed by remineralization of organic matter and nitrification, while the strong correlation between AOU and $\Delta\text{N}_2\text{O}$ commonly observed in depth profiles provides circumstantial evidence that

nitrification is the dominant mechanism of N_2O production in oceans (Nevison et al. 2003), lakes (Mengis et al. 1996; Wang et al. 2009), and reservoirs (Mengis et al. 1997; Liu et al. 2011). The reported regression coefficient varies from 0.076 to 0.31 $\text{nmol L}^{-1} \Delta\text{N}_2\text{O}/\mu\text{mol L}^{-1} \text{AOU}$ (Suntharalingam and Sarmiento 2000).

In Fig. 7, $\Delta\text{N}_2\text{O}$ was plotted versus AOU for all water samples throughout the reservoir. While a considerable amount of scatter appears on the figure, significant positive correlation between AOU and $\Delta\text{N}_2\text{O}$ was found in the sampling year with the exception of spring. A good linear correlation was found in summer ($R = 0.75$; $P = 0.001$; July to September) in DFR; the calculated regression coefficient was 0.19 $\text{nmol L}^{-1} \Delta\text{N}_2\text{O}/\mu\text{mol L}^{-1} \text{AOU}$. A significant positive correlation between AOU and $\Delta\text{N}_2\text{O}$ was also found in the cold season ($R = 0.41$; $P = 0.023$; October to March), with a calculated regression coefficient of 0.23 $\text{nmol L}^{-1} \Delta\text{N}_2\text{O}/\mu\text{mol L}^{-1} \text{AOU}$. The regression coefficients for reservoirs in this study agree nicely with reported coefficients in lakes and oceans (Mengis et al. 1997; Nevison et al. 2003; Wang et al. 2009; Liu et al. 2011), indicating that N_2O production in DFR was

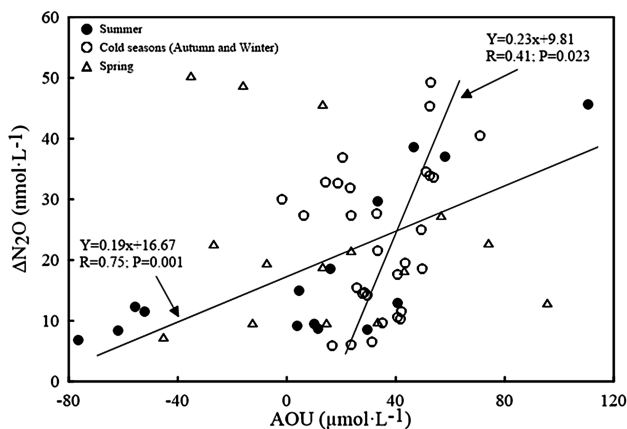


Fig. 7 $\Delta\text{N}_2\text{O}$ versus AOU in Dongfeng reservoir

predominated by nitrification. In addition, even though N_2O only correlated with NO_3^- in autumn, it exhibited a wide-ranging positive correlation with NH_4^+ , which supports N_2O production by nitrification.

This approach for identifying the key process of N_2O production is not definitive as numerous factors can contribute to the variability (Mengis et al. 1997). Organic matter that oxidized in different layers, or differences in the production yield of nitrifiers could result in varying $\Delta\text{N}_2\text{O}/\text{AOU}$ ratios. In addition, mixing of different water masses or additional N_2O sources, such as denitrification or assimilative NO_3^- reduction, may also affect $\Delta\text{N}_2\text{O}/\text{AOU}$ ratios.

4.3 $\text{N}_2\text{O-N}:\text{NO}_3\text{-N}$ ratio for assessing N_2O production and IPCC methodology

The IPCC method for indirect N_2O emissions assumes that a certain proportion of soil nitrogen including anthropogenic fertilizer and organic nitrogen is leached to aquatic ecosystems, from which N_2O is produced and emitted from groundwater and surface drainages to rivers and estuaries (IPCC 2006). Indirect N_2O emissions from agricultural N utilization are estimated for groundwater, rivers, and estuaries using an emission factor (EF5) for aquatic ecosystems. Currently, EF5 is set at 0.75% (kg $\text{N}_2\text{O-N}$ per kg N leached), with an uncertainty range of 0.05%–2.5% (IPCC 2006). Specifically, for each aquatic component, the aquatic EF5 values are currently 0.25% for groundwater and surface drainage (EF5-g), rivers (EF5-r), and estuaries (EF5-e) (IPCC 2006; Baulch et al. 2012). Recently, the IPCC method for estimating indirect N_2O emissions from aquatic systems came into dispute (Baulch et al. 2012; Hinshaw and Dahlgren 2013; Yu et al. 2013). The current EF5-r value was confirmed based on data primarily from

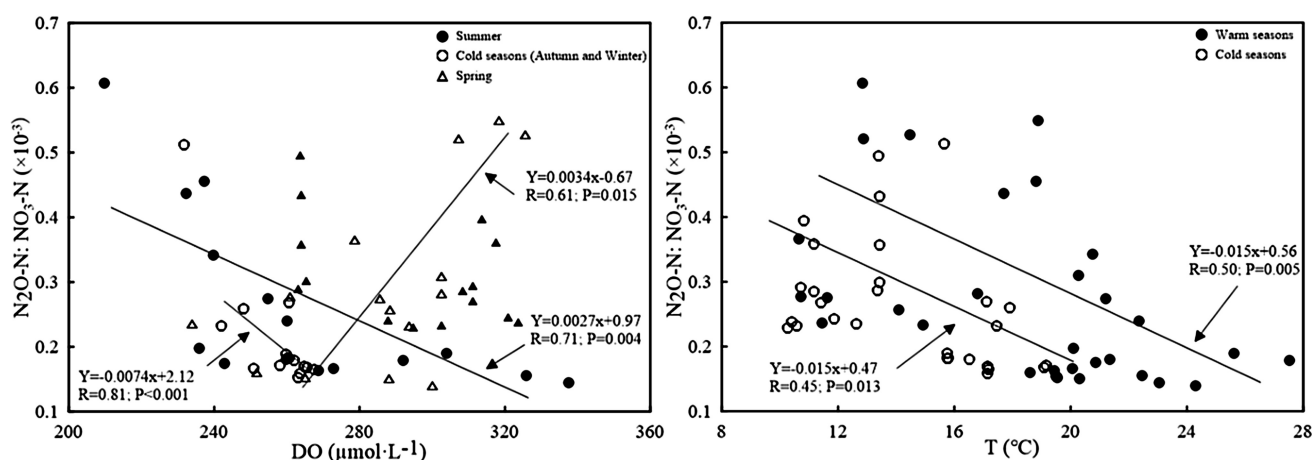
small river systems, but there remains great uncertainty in scaling these values to larger rivers (Hinshaw and Dahlgren 2013). Studies in Ohio rivers showed a three-fold overestimation of N_2O (Beaulieu et al. 2011), and in spring-fed rivers in New Zealand, only 0.01% of N_2O estimated by IPCC methodology was observed (Clough et al. 2007). This uncertainty could be even greater for impounded rivers with multiple reservoirs.

Ratios of dissolved $\text{N}_2\text{O-N}:\text{NO}_3\text{-N}$ from groundwater and agricultural drainage water has been used to confirm the EF5 value; in many studies this ratio has been used directly to evaluate emissions in rivers and lakes (McCrackin and Elser 2011), but few studies have focused on reservoirs. The $\text{N}_2\text{O-N}:\text{NO}_3\text{-N}$ ratio in DFR over the study year ranged from 1.4×10^{-4} to 6.1×10^{-4} , with an average value of 2.7×10^{-4} , much lower than the default EF5 value of 75×10^{-4} , and even above the minimum value of 5×10^{-4} , suggesting an overestimation by IPCC methodology for reservoirs. Table 1 compares $\text{N}_2\text{O-N}:\text{NO}_3\text{-N}$ ratios presented in recent literature. $\text{N}_2\text{O-N}:\text{NO}_3\text{-N}$ ratios in HJD, WJD, and DFR along the Wujiang River exhibited lower values than default ratio values from IPCC methodology, suggesting that N_2O fluxes from reservoirs in Wujiang River would be significantly overestimated by the IPCC method. Similar overestimate would also happen in Swiss reservoirs (Mengis et al. 1997) and in Taihu Lake in China (Wang et al. 2009), where $\text{N}_2\text{O-N}:\text{NO}_3\text{-N}$ ratios averaged 0.002 (Fig. 1). However, for reservoirs in the United States and Finland, default IPCC values would lead to an underestimate (Huttunen et al. 2002; Deemer et al. 2011).

The $\text{N}_2\text{O-N}:\text{NO}_3\text{-N}$ ratios vary substantially among different reservoirs worldwide, contributing to poor understanding of N_2O emissions and spatiotemporal patterns, e.g. how the ratio of $\text{N}_2\text{O-N}:\text{NO}_3\text{-N}$ varies seasonally and vertically within a reservoir is still unknown and the key influencing factors still not well understood. Significant negative correlation was observed between $\text{N}_2\text{O-N}:\text{NO}_3\text{-N}$ ratios and T throughout the year in DFR ($R = 0.45$; $P = 0.013$ in cold season; $R = 0.50$; $P = 0.005$ in warm season) (Fig. 8). T seemed to constrain N_2O formation by NO_3^- in the reservoir. However, DO displayed a much more complicated seasonal variation. Negative correlation was observed in summer ($R = 0.71$; $P = 0.004$) and winter and autumn ($R = 0.81$; $P < 0.001$) (Fig. 8). Nitrification was recognized as the dominant process for N_2O production in DFR and a positive correlation between $\text{N}_2\text{O-N}:\text{NO}_3\text{-N}$ ratios and DO was observed in spring, indicating that DO increases $\text{N}_2\text{O-N}:\text{NO}_3\text{-N}$ ratios. Further research is needed to confirm this relationship.

Table 1 Comparison of the ratio of $\text{N}_2\text{O-N}:\text{NO}_3\text{-N}$ among different studies

Name of lake/reservoir	Location	Ratio of $[\text{N}_2\text{O-N}]:[\text{NO}_3\text{-N}]$		References
		Average	Range	
Dongfeng reservoir	China	0.00027	0.0001–0.0006	This study
Wujiangdu reservoir	China	0.00040	0.00017–0.0014	Liu et al. (2011a)
Hongjiadu reservoir	China	0.00045	0.00014–0.0031	Liu et al. (2011a)
26 lakes in Colorado	USA	0.01	0.001–0.07	McCrackin and Elser (2011)
Lacamas reservoir	USA	0.009	0.002–0.02	Deemer et al. (2011)
Taihu Lake	China	0.002	0.0003–0.02	Wang et al. (2009)
Lokaa reservoir	Finland	0.026	0.004–0.031	Huttunen et al. (2002)
Greifensee	Switzerland	0.002	0–0.017	Mengis et al. (1997)
IPCC indirect N_2O emission factor (EF5)	N/A	0.0025	0.0005–0.025	IPCC (2006)

**Fig. 8** Relationship between $\text{N}_2\text{O-N}:\text{NO}_3\text{-N}$ ratios and T, DO

4.4 N_2O emission fluxes compared with other water bodies

Exchange fluxes of N_2O were estimated in DFR by month, as previously noted; maximum and minimum emission fluxes values were in April 2008 and October 2007, respectively. In April (early stage of thermal stratification), N_2O emission was expected to exhibit a supersaturation status and high emission flux, as found in other reservoirs (Liu et al. 2011a; Beaulieu et al. 2014), but this temporal pattern was complicated by variable nitrogen dynamics, especially in thermal stratification seasons. N_2O fluxes of other reservoirs and lakes worldwide are listed in Table 2. Tropical reservoirs tend to emit more N_2O through the water–air interface than subtropical and temperate reservoirs. In addition, DFR had rather low N_2O emission flux when compared to other subtropical reservoirs, including the adjacent WJD and HJD reservoirs. As many lakes and reservoirs worldwide, those in the Wujiang basin are subject to substantial N loading from the surrounding

watershed as evidenced by the high N levels in HJD, WJD, and DFR. Even though DFR is a mesotrophic reservoir, the N_2O production and saturation in the hyperlimnion maintained a high level when compared with the eutrophic WJD reservoir. However, the difference in N_2O emission fluxes between WJD and DFR indicates that nutrient status impacts N_2O production.

According to the N_2O emission fluxes and water surface area of DFR (19.06 km²), we estimated the annual N_2O emissions from the water–air interface to be 0.32×10^5 mol N_2O . Due to a smaller water surface area and flux, annual N_2O emissions were less in DFR than in HJD and WJD (3.17×10^5 mol N_2O and 2.81×10^5 mol N_2O , respectively) (Liu et al. 2011a). Although this annual N_2O emission amount was not comparable with large rivers and soil systems, it should be emphasized since most rivers worldwide are impounded with reservoirs, especially in China. China is already the world's largest producer of hydroelectricity, with more than 220 large- and medium-scale (>50 MW) hydropower plants and over 40,000

Table 2 Emission fluxes of N₂O at water–air interface in lakes and reservoirs

Name	Location	Climate	FN ₂ O (μmol m ⁻² h ⁻¹)	References
Reservoirs				
Petit Saut	French Guiana	Tropical	4.04 ± 2.54	Guerin et al. (2008)
Fortuna	Panama	Tropical	0.29 ± 0.46	Guerin et al. (2008)
Tucuruí	Brazil	Tropical	5.21 ± 3.42	Lima et al. (2002)
Samuel	Brazil	Tropical	6.54 ± 6.17	Lima et al. (2002)
Serra de Mesa	Brazil	Tropical	0.13 ± 0.92	Sikar et al. (2005)
Manso	Brazil	Tropical	0.13 ± 1.25	Sikar et al. (2005)
William H. Harsha	United States	Extratropical	≈ −50 ~ ≈ 100 (data from fig)	Beaulieu et al. (2014)
Lokka	Finland	Temperate	−0.08 ~ 0.26	Huttunen et al. (2002)
Porttipahta	Finland	Temperate	−0.02 ~ 0.24	Huttunen et al. (2002)
Three Gorges	China	Subtropical	0.32 ± 0.48	Zhu et al. (2013)
Hongjiadu	China	Subtropical	0.45 (0.10 ~ 1.32)	Liu et al. (2011a)
Wujiangdu	China	Subtropical	0.64 (0.08 ~ 1.76)	Liu et al. (2011a)
Dongfeng	China	Subtropical	0.19 (0.01 ~ 0.61)	This study
Natural lakes				
Mochou	Antarctica	Frigid	0.22 ± 0.48	Liu et al. (2011b)
Tuanjie	Antarctica	Frigid	0.18 ± 0.20	Liu et al. (2011b)
Daming	Antarctica	Frigid	0.51 ± 0.49	Liu et al. (2011b)
ELA in Ontario	Canada	Temperate	<0.0033	Hendzel et al. (2005)
Kevaton	Finland	Temperate	0.09 ~ 0.50	Huttunen et al. (2003)
Tahu	China	Subtropical	0.41–0.58	Wang et al. (2009)
Yuqiao	China	Subtropical	0.18 (−0.14 to 0.89)	Liu et al. (2015)

smaller-scale ones. Given the rate of dam construction, GHG emissions from hydroelectric reservoirs may have significant global impact (Hu and Cheng 2013).

In addition, supersaturated N₂O content in the bottom waters will be released into the atmosphere as water passing through the turbines and spillways is drawn from the lower layer, and downstream GHG emissions will occur as water is released under pressure below the dam (Liu et al. 2011a; Fearnside and Pueyo 2012). In 2007, the water output of DFR was about 5.02×10^9 m³, and the average concentration of N₂O in discharged water was 31.04 nmol L⁻¹. In total, 1.56×10^5 mol N₂O was released through power generation, which is nearly five times the N₂O emissions from the water–air interface. A similar difference between N₂O degassing from water–air interface and releasing water during power generation was found in WJD and HJD, but DFR has the highest proportion of the three. This is mainly because DFR has larger output than the other two reservoirs, demonstrating that management of reservoir operations strongly affects N₂O degassing.

The annual electric energy production of DFR is 24.2×10^8 kW/h (<http://192.168.4.1/gsgk/zjdz/3213.htm>). Combined N₂O emissions from the water–air interface and degassing from releasing water during power generation was

1.88×10^5 mol N₂O. So, per 1 kW/h electrical power, DFR released 77.69 μmol N₂O, which was lower than both WJD and HJD (107.78 and 134.88 μmol/kW/h, respectively).

5 Conclusions

This study investigated the temporal and spatial variation of N₂O as well as controlling factors in a mesotrophic reservoir. Though as a mesotrophic reservoir, DFR acted as obvious N₂O sources with respect to atmosphere. However, N₂O emission fluxes in DFR were significantly lower than that in the neighboring eutrophic WJD reservoir, implying that eutrophication may enhance the N₂O emission. N₂O production in DFR was dominated by nitrification in well-oxygenated water layers, while no obvious effects of denitrification on N₂O emission were observed in DFR, which should be emphasized in future researches, especially in sediment–water interface.

IPCC methodology would seemingly lead to overestimation if it were applied in reservoirs of the Wujiang River, but this needs to be substantiated by further observation because it remains unclear 1) how seasonal and diurnal N₂O variation influence N₂O-N: NO₃-N ratios and

2) how some special events, such as ice-cover water, may affect N_2O production with respect to NO_3^- .

N_2O emission flux from the water–air interface and N_2O degassing from releasing water behind the dam during power generation should be given equal attention and emphasis. N_2O emission flux from surface waters is related to N_2O saturation and physical–chemical quality, while N_2O degassing during power generation is related to water output and N_2O saturation in releasing water layers.

Acknowledgements This study was financially supported by the National Key Research and Development Program of China through grant 2016YFA0601000; the National Major Scientific Research Program Grant No. 2013CB956401; the National Natural Science Foundation of China through Grants Nos. 41325010, 41403082, and 41302285; and the Tianjin Research Program of Application Foundation and Advanced Technology Grant No. 14JCQNJC08800. We are grateful to Shi-Lu Wang, Ning An, and anonymous reviewers for valuable comments and suggestions on this manuscript.

Compliance with ethical standards

Conflict of interest The authors declare that they have no conflicts of interest to this work. We declare that we do not have any commercial or associative interest that represents a conflict of interest in connection with the work submitted.

References

- Baulch HM, Schiff Sherry L, Maranger R, Dillon Peter J (2012) Testing models of aquatic N_2O flux for inland waters. *Can J Fish Aquat Sci* 69:145–160
- Beaulieu JJ, Tank JL, Hamilton SK, Wollheim WM, Hall RO, Mulholland PJ, Peterson BJ, Ashkenas LR, Cooper LW, Dahm CN, Dodds WK, Grimm NB, Johnson SL, McDowell WH, Poole GC, Valett HM, Arango CP, Bernot MJ, Burgin AJ, Crenshaw CL, Helton AM, Johnson LT, O'Brien JM, Potter JD, Sheibley RW, Sobota DJ, Thomas SM (2011) Nitrous oxide emission from denitrification in stream and river networks. *Proc Natl Acad Sci USA* 108:214–219
- Beaulieu JJ, Smolenski RL, Nietch CT, Townsend-Small A, Elovitz MS, Schubauer-Berigan JP (2014) Denitrification alternates between a source and sink of nitrous oxide in the hypolimnion of a thermally stratified reservoir. *Limnol Oceanogr* 59:495–506
- Beaulieu JJ, Nietch CT, Young JL (2015) Controls on nitrous oxide production and consumption in reservoirs of the Ohio River Basin. *J Geophys Res Biogeosci* 120:1995–2010
- Clough TJ, Buckthought LE, Kelliher FM, Sherlock RR (2007) Diurnal fluctuations of dissolved nitrous oxide (N_2O) concentrations and estimates of N_2O emissions from a spring-fed river: implications for IPCC methodology. *Glob Change Biol* 13:1016–1027
- Deemer BR, Harrison JA, Whitling EW (2011) Microbial dinitrogen and nitrous oxide production in a small eutrophic reservoir: an in situ approach to quantifying hypolimnetic process rates. *Limnol Oceanogr* 56:1189–1199
- Emerson S (1975) Chemically enhanced CO_2 gas exchange in a eutrophic lake: a general model. *Limnol Oceanogr* 20:743–753
- Fearnside PM (2016) Greenhouse gas emissions from Brazil's Amazonian hydroelectric dams. *Environ Res Lett* 11: 011002. doi:10.1088/1748-9326/11/1/011002
- Fearnside PM, Pueyo S (2012) Greenhouse-gas emissions from tropical dams. *Nature Clim Change* 2:382–384
- Guerin F, Abril G, Tremblay A, Delmas R (2008) Nitrous oxide emissions from tropical hydroelectric reservoirs. *Geophys Res Lett* 35:L06404. doi:10.1029/2007GL033057
- Han G, Tang Y, Xu Z (2010) Fluvial geochemistry of rivers draining karst terrain in Southwest China. *J Asian Earth Sci* 38:65–75
- Hendzel LL, Matthews CJD, Venkiteswaran JJ, Louis VLS, Burton D, Joyce EM, Bodaly RA (2005) Nitrous oxide fluxes in three experimental boreal forest reservoirs. *Environ Sci Technol* 39:4353–4360
- Hinshaw SE, Dahlgren RA (2013) Dissolved nitrous oxide concentrations and fluxes from the eutrophic San Joaquin River, California. *Environ Sci Technol* 47:1313–1322
- Hu Y, Cheng H (2013) The urgency of assessing the greenhouse gas budgets of hydroelectric reservoirs in China. *Nature Clim Change* 3:708–712
- Huttunen JT, Vaisanen TS, Hellsten SK, Heikkinen M, Nykanen H, Jungner H, Niskanen A, Virtanen MO, Lindqvist OV, Nenonen OS, Martikainen PJ (2002) Fluxes of CH_4 , CO_2 , and N_2O in hydroelectric reservoirs Lokka and Porttipahta in the northern boreal zone in Finland. *Glob Biogeochem Cycles*. doi:10.1029/2000GB001316
- Huttunen JT, Juutinen S, Alm J, Larmola T, Hammar T, Silvola J, Martikainen PJ (2003) Nitrous oxide flux to the atmosphere from the littoral zone of a boreal lake. *J Geophys Res Atmos* 108:4421. doi:10.1029/2002JD002989
- IPCC (2006) IPCC guidelines for national greenhouse gas inventories. Prepared by the National Greenhouse Gas Inventory Program. Institute for Global Environmental Strategies, Hayama
- Lerman A (1979) Geochemical processes. Water and sediment environments. John Wiley and Sons, Inc., Hoboken
- Li SL, Liu CQ, Li J, Liu XL, Chetelat B, Wang BL, Wang FS (2010) Assessment of the sources of nitrate in the Changjiang River, China using a nitrogen and oxygen isotopic approach. *Environ Sci Technol* 44:1573–1578
- Lima Id, Victoria R, Novo E, Feigl B, Ballester M, Ometto J (2002) Methane, carbon dioxide and nitrous oxide emissions from two Amazonian reservoirs during high water table. *Internationale Vereinigung fur Theoretische und Angewandte Limnologie Verhandlungen* 28:438–442
- Liu CQ (2007) Biogeochemical processes and cycling of nutrients in the earth's surface: chemical erosion and nutrient cycling in Karstic catchments, Southwest China. Science Press, Beijing, p 608 (in Chinese)
- Liu XL, Liu CQ, Li SL, Wang FS, Wang BL, Wang ZL (2011a) Spatiotemporal variations of nitrous oxide (N_2O) emissions from two reservoirs in SW China. *Atmos Environ* 45:5458–5468
- Liu Y, Zhu R, Ma D, Xu H, Luo Y, Huang T, Sun L (2011b) Temporal and spatial variations of nitrous oxide fluxes from the littoral zones of three alga-rich lakes in coastal Antarctica. *Atmos Environ* 45:1464–1475
- Liu XL, Bai L, Wang ZL, Li J, Yue FJ, Li SL (2015) Nitrous oxide emissions from river network with variable nitrogen loading in Tianjin, China. *J Geochem Explor* 157:153–161
- McCrackin ML, Elser JJ (2011) Greenhouse gas dynamics in lakes receiving atmospheric nitrogen deposition. *Glob Biogeochem Cycles* 25:GB4005. doi:10.1029/2010GB003897
- Mengis M, Gachter R, Wehrli B (1996) Nitrous oxide emissions to the atmosphere from an artificially oxygenated lake. *Limnol Oceanogr* 41:548–553
- Mengis M, Gachter R, Wehrli B (1997) Sources and sinks of nitrous oxide (N_2O) in deep lakes. *Biogeochemistry* 38:281–301
- Musenze RS, Fan L, Grinham A, Werner U, Gale D, Udy J, Yuan ZG (2016) Methane dynamics in subtropical freshwater reservoirs

- and the mediating microbial communities. *Biogeochemistry* 128:233–255
- Nevison C, Butler JH, Elkins JW (2003) Global distribution of N_2O and the Delta N_2O -AOU yield in the subsurface ocean. *Glob Biogeochem Cycles* 17:1119. doi:10.1029/2003GB002068
- Peng X, Wang B, Liu C, Liu X, Wang F (2012) Diurnal variations of pCO_2 in relation to environmental factors in the cascade reservoirs along the Wujiang River, China. *Chin J Geochem* 31:41–47
- Ravishankara AR, Daniel JS, Portmann RW (2009) Nitrous Oxide (N_2O): the dominant ozone-depleting substance emitted in the 21st century. *Science* 326:123–125
- Rosenberg DM, McCully P, Pringle CM (2000) Global-scale environmental effects of hydrological alterations: introduction. *Bioscience* 50:746–751
- Sasaki Y, Koba K, Yamamoto M, Makabe A, Ueno Y, Nakagawa M, Toyoda S, Yoshida N, Yoh M (2011) Biogeochemistry of nitrous oxide in Lake Kizaki, Japan, elucidated by nitrous oxide isotopomer analysis. *J Geophys Res Biogeosci* 116
- Satterfield CN (1970) Mass transfer in heterogeneous catalysis. MIT Press, Cambridge
- Seitzinger SP, Kroeze C (1998) Global distribution of nitrous oxide production and N inputs in freshwater and coastal marine ecosystems. *Global Biogeochem Cycles* 12:93–113
- Sikar E, Santos M, Matvienko B, Silva M, Rocha C, Santos E, Bentes A, Rosa L (2005) Greenhouse gases and initial findings on the carbon circulation in two reservoirs and their watersheds. *Proc Int Assoc Theor Appl Limnol* 29:573
- Sturm K, Yuan Z, Gibbes B, Werner U, Grinham A (2014) Methane and nitrous oxide sources and emissions in a subtropical freshwater reservoir, South East Queensland, Australia. *Biogeochemistry* 11:5245–5258
- Suntharalingam P, Sarmiento JL (2000) Factors governing the oceanic nitrous oxide distribution: simulations with an ocean general circulation model. *Global Biogeochem Cycles* 14:429–454
- Wang SL, Liu CQ, Yeager KM, Wan GJ, Li J, Tao FX, Lue YC, Liu F, Fan CX (2009) The spatial distribution and emission of nitrous oxide (N_2O) in a large eutrophic lake in eastern China: anthropogenic effects. *Sci Total Environ* 407:3330–3337
- Wang F, Wang B, Liu C-Q, Wang Y, Guan J, Liu X, Yu Y (2011) Carbon dioxide emission from surface water in cascade reservoirs-river system on the Maotiao River, southwest of China. *Atmos Environ* 45:3827–3834
- Wang SL, Yeager K, Wan GJ, Liu CQ, Liu F, Lu YC (2015) Dynamics of CO_2 in a karst catchment in the southwestern plateau, China. *Environ Earth Sci* 73:2415–2427
- Yu ZJ, Deng HG, Wang DQ, Ye MW, Tan YJ, Li YJ, Chen ZL, Xu SY (2013) Nitrous oxide emissions in the Shanghai river network: implications for the effects of urban sewage and IPCC methodology. *Glob Change Biol* 19:2999–3010
- Zhu D, Chen H, Yuan X, Wu N, Gao Y, Wu Y, Zhang Y, Peng C, Qa Zhu, Yang G, Wu J (2013) Nitrous oxide emissions from the surface of the Three Gorges Reservoir. *Ecol Eng* 60:150–154